Available online at www.sciencedirect.com

SciVerse ScienceDirect

journal homepage: www.elsevier.com/locate/he

Glycerol steam reforming in a bench scale continuous flow heat recovery reactor

André Valente Bueno [a,*], Mona Lisa Moura de Oliveira [b]

[a] Mechanical Engineering Department, Federal University of Ceara, CEP 60455-760 Fortaleza, CE, Brazil
[b] Mechanical Engineering Department, University of Fortaleza, CEP 60811-905 Fortaleza, CE, Brazil

ARTICLE INFO

Article history:
Received 4 May 2013
Received in revised form
18 July 2013
Accepted 19 August 2013
Available online 14 September 2013

Keywords:
Biodiesel
Glycerol
Steam reforming
Heat recovery reactor

ABSTRACT

In the present study glycerol was successfully gasified using a diesel engine waste heat recovery system obtaining hydrogen and methane rich gaseous products. The reforming reactor was equipped with a vaporization pre-chamber to ensure uniform reactants distribution and a fixed reaction bed, being mounted in countercurrent flow configuration with the engine combustion gases stream. Accordingly, the reactions were conducted at gradually increased temperature conditions; starting at around 300 °C in the top section of the reaction bed and finishing in a controlled outlet bed temperature of 600–800 °C. When compared to homogeneous temperature reactors, the configuration used here produced a syngas of higher methane and ethylene contents. With regards to the reactor performance, syngas lower heat values of more than 22 MJ/kg were achieved with glycerol feed concentrations within 50–70% and outlet bed temperatures above 700 °C, corresponding to cold gas efficiencies of around 85%. The present results indicate that glycerin can be utilized as a syngas feedstock for steam reforming processes based on waste heat recovery.

1. Introduction

The esters of biological fats or oils, also known as biodiesel, have been regarded as promising renewable substitutes for mineral diesel fuel [1–3]. Biodiesel industrial production generally includes a transesterification step where triglycerides react with an alcohol, yielding value added esters and glycerol as a by-product. This glycerol is a low price unrefined substance that contains contaminants such as salts, catalysts and methanol whose removal constitutes an economically unfeasible activity. Since the majority of industrial processes require purified or distilled glycerol as raw material, unrefined glycerol derived from the emergent biodiesel industry has become a potential environmental pollutant [4]. For the year of 2013, for instance, a surplus of 150,000 tons of glycerol is expected only in the Brazilian market due to biodiesel production.

In response to this scenario, alternatives for the use of unrefined glycerol in the production of value-added chemicals [5,6], automotive fuels [7,8] and hydrogen [9–11] have received special attention. The environmental benefits of making use of waste glycerol can be enhanced with its conversion to a hydrogen and methane rich gas via a near carbon-neutral process, since fossil fuels are the present dominant source of industrial hydrogen and syngas. Accordingly, several thermochemical processes have been studied in order to obtain renewable hydrogen from glycerol: steam reforming [12–17]; autothermal steam reforming [18]; pyrolysis or partial oxidation [15,19]; aqueous-phase reforming [20,21]; supercritical water reforming [22–24]. Selected results from these works are summarized in Table 1.

* Corresponding author. Tel.: +55 85 33669638; fax: +55 85 33669636.
E-mail address: bueno@ufc.br (A.V. Bueno).
0360-3199/$ – see front matter
http://dx.doi.org/10.1016/j.ijhydene.2013.08.082

Using a laminar flow reactor, Jones and co-workers [12] analyzed the thermal decomposition of glycerol in steam at 650–700 °C. They identified carbon monoxide, acetaldehyde, acrolein, hydrogen, ethylene, methane, ethane and carbon dioxide as the main decomposition products with short residence times of about one tenth of second. Valliyappan et al. [13] carried the steam reforming of glycerol with residence times in the order of 2 s and a temperature of 800 °C. These authors employed a uniformly heated reactor carried with Ni/Al_3O_2 catalyst to produce syngas with up to 68.4% mol of hydrogen, at a steam to glycerol feed ratio of 25:75. Adhikari and co-workers [14] obtained syngas with 56.5% of hydrogen operating a catalytic (Ni/MgO) open flow reactor at 800 °C. A tube furnace was employed to sustain the reforming reactions. Fernandez et al. [15] used a carbonaceous catalyst to produce syngas with up to 40.9% of hydrogen and 10.8% of methane, maintaining the reforming reactions at 650 °C with a microwave assisted device. Atong and co-researchers [16] tested olivine-supported nickel catalysts as active in-bed materials for steam reforming of glycerol waste, obtaining a product gas with 22% of hydrogen and 50% of methane. Douette et al. [17] investigated the impact of the operational parameters oxygen to carbon ratio, steam to carbon ratio and temperature upon glycerol reforming. These authors employed an open flow reactor filled with nickel-based catalyst, which was mounted inside a furnace. A maximum outlet hydrogen concentration of 60.4% was obtained with a glycerol/water feed ratio of 1:9 and a temperature of 804 °C. In a general view, steam reforming of glycerol has been successfully conduced at atmospheric pressure in small-scale uniformly heated reactors, within a temperature range from 700 to 1000 °C and reactants concentrations of around one part of glycerol and one part of water, in weight basis. Values of about 85% have been reported for the gas yield, gasification efficiency or reforming efficiency, usually defined as the mass of dry syngas obtained per kilogram of glycerol that enters the reactor. Hydrogen, in molar concentrations from 22 to 68%, and methane, in concentrations from 13 to 4%, predominated among the gaseous products.

Hydrogen concentrations from 36 up to 70% and a practically unitary gas yield have been achieved with the supercritical water reforming method, which on the other hand demands high pressure reactors. A complex setup is necessary to sustain the reactor conditions in a pressure range from 25,000 to 35,000 kPa and temperatures above 510 °C after the supercritical media distinctive properties; low viscosity, high diffusivity and low dielectric constant. Conversely, similar results were previously obtained by Dumesic and co-workers [9,20,21] with aqueous-phase reforming in subcritical conditions, namely at 265 °C and 5140 kPa. Dumesic et al. proposed the catalytic reforming of biomass-derived hydrocarbons in liquid water by observing a remarkable characteristic of these substances: they can be thermally decomposed in temperatures substantially lower when compared to their equivalent alkanes or alkenes [9]. As can be seen in Fig. 1, steam reforming of glycerol is thermodynamically favorable from 60 °C, while for its alkane counterpart C_3H_8, it becomes thermodynamically favorable only from 440 °C. In fact, the practical limit to initiate the gaseous phase reforming of glycerol at atmospheric pressure is the vaporization temperature of the reactants mixture whilst, at least theoretically, a low temperature waste heat source can successfully drive the early stages of this type of decomposition process.

From this brief literature review, it is evident that there has been significant amount of effort to cover the operational effects of temperature, pressure, catalytic bed

Table 1 – A summary of the thermochemical processes proposed for obtaining hydrogen and/or methane from glycerol.

Process/reference		Reactor				Reactants			Products			
		Operational conditions				Concentration [%mol]			Concentration [%mol]			Gas [%wt]
		Bed type	T [C]	P [kPa]	t [s]	$C_3H_8O_3$	H_2O	Gas	H_2	CH_4	CO	
Steam reforming	[12]	Open flow	700	101.3	0.1	1.0	99	–	33.0	8.3	43.5	4.4
	[13]	Fixed bed	800	101.3	2.0	16.4	83.6	–	54.1	7.4	37.5	94.0
Catalytic steam reforming	[13]	Fixed bed	800	101.3	2.0	16.4	83.6	–	68.2	4.1	19.9	89.6
	[14]	Open flow	650	101.3	3.4	14.3	85.7	–	56.5			86.6
	[15]	Fixed bed	800	101.3	2.3	16.4	83.6	–	40.9	10.8	44.0	68.1
	[16]	Fixed bed	800	101.3	0.4	18.5	14.8	66.7 N_2	22.0	50.0	20.0	84.0*C
	[17]	Open flow	804	101.3	1.0	10.4	89.6	–	60.4	1.3	18.8	
Autothermal steam reforming	[18]	Entrained flow	1000	101.3	32.6	15.2	9.1	51.9 Air	40	4	39	85.0
Pyrolysis	[19]	Fixed bed	800	101.3	2.9	13.2	–	86.8 N_2	48.6	3.3	44.9	66.6
Catalytic pyrolysis	[15]	Fixed bed	800	101.3	2.3	79.0	–	21.0 N_2	34.6	13.5	45.9	83.6
Catalytic aqueous-phase reforming	[20]	Fixed bed	265	5600	8836	1.0	99.0	–	54.0	6.0	0.0	99.0*C
	[21]	Fixed bed	265	5140	2195	1.0	99.0	–	62.0	7.0	0.0	99.0*C
Supercritical water reforming	[23]	Open flow	500	25,000	58.8	0.2	99.8	–	63.5	7.5	1.5	98.0
	[24]	Fixed bed	550	35,000	8	1.0	99.0	–	27.5	17.0	22.3	100.0
	[25]	Open flow	567	25,000	5.8	2.1	97.9	–	59.3	3.4	18.0	88.0
	[25]	Open flow	567	25,000	5.8	16.4	83.6	–	52.0	5.0	30.0	72.0
Catalytic sup. water reforming	[22]	Fixed bed	800	24,100	1	1.0	99	–	70.0	3.7	1.1	
	[22]	Fixed bed	800	24,100	1	11.5	88.5	–	40.2	18.9	4.3	
	[24]	Fixed bed	510	35,000	8	1.0	99.0	–	36.0	13.3	25.1	100.0

*C carbon balance data.

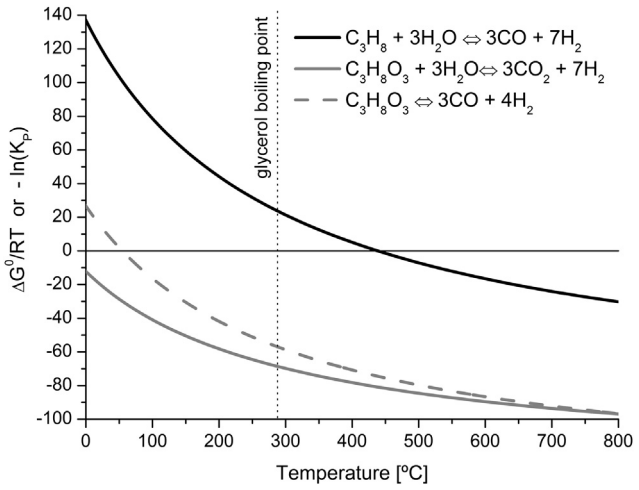

Fig. 1 – $\Delta G^0/RT$ versus temperature for production of CO and H_2 from vapor phase reforming of $C_3H_8O_3$ and C_3H_8. Adapted from [9].

materials and reactants concentrations upon reforming indicators such as the reforming efficiency and the gaseous products composition. Conversely, aspects like the impact of the above mentioned operational parameters over the reactor energy balance and the integration of the reforming process with industrial heat sources remain particularly unexplored. In fact, external electrical heating and nearly homogeneous bed temperatures without any mention to energy efficiency aspects predominated among the selected references, the only exception being the work of Yoon et al. where a maximum cold gas efficiency of 65% was reported for air blown gasification [18]. Gaseous products composition and energy analysis data for a glycerol reforming process based on waste heat recovery also have yet to be addressed in detail.

The aim of the present work is to investigate the heat exchange between the reaction bed and a power cycle effluent as an alternative to conduct the glycerol reforming with enhanced heat integration and energy efficiency. The particular characteristic of being thermodynamically feasible at low temperatures makes glycerol steam reforming especially attractive to this kind of application. Accordingly, this thermal decomposition process was successfully conducted with a bench-scale shell and tube heat recovery reactor operating in conjunction with a diesel engine. A non-catalytic fixed porous bed mounted inside one tube pass was employed as reaction medium. In order to avoid excessive char formation owing to uneven reactants distribution, the glycerol/water feed was evaporated inside a low temperature pre-chamber, while the decomposition reactions eventually proceeded in a bed of progressively increased temperature, by extracting heat from a countercurrent flow of engine exhaust hot gases. The effects of glycerol feed concentration and reaction temperature upon the gas products yield, composition and cold gas efficiency were systematically addressed by means of steady-state experiments. Glycerol concentration was varied from 10 to 90% in weight basis within reactor outlet temperatures ranging from 600 to 800 °C.

2. Materials and methods

Steam reforming of glycerol (99.5% purity) was continuously performed in a heat recovery reactor with the purpose of obtaining products suitable for use as a fuel. An assembly design of the apparatus used in the experiments is provided in Fig. 2.

Glycerol/water mixture was introduced in the reactor by a liquid cooled head, entering a bowl-shaped evaporation chamber. After evaporated, the reactants passed to the reaction zone through a series of orifices that surround the evaporation bowl. The glycerol steam reforming took place in a cylindrical fixed bed with 94 mm of internal diameter and 531 mm of height, receiving heat from the reactor shell that was in direct contact with combustion products. High purity alumina (Al_2O_3) spheres with 1.5 mm of diameter were adopted as the packing material. Before leaving the reactor, the reforming products crossed an orifice plate at the bottom of the fixed bed, which was adopted after several obstructions of the outlet tube by the packing material.

The energy required for the reforming reactions was recuperated from combustion gases exhausted by an air cooled single cylinder diesel engine (see Table 2 for specifications). In maximum load conditions, which correspond to 3694 rpm and 4.25 kW of brake power, the engine delivered 38.69 kg/h of combustion gases at 914 °C. In regard to endure such temperatures, the reforming reactor and the liquid separator were made of AISI 310 stainless steel. A ceramic insulation sleeve prevented heat losses from the combustion gases circuit to the surroundings.

Five shell configurations with 11, 21, 31, 41, and 51 baffles were tested for the hot flow side. Within this inquiry, experiments were conduced with combustion gases entering the reactor at 700 °C and 1:1 glycerol/water mixture, by weight, being continuously injected at 44 ml/min. The results obtained for the engine exhaust back pressure and reactor outlet temperature are reported in Fig. 3. The configuration corresponding to 21 shell baffles was adopted here, since it exhibited the best compromise between reactor outlet temperature and combustion gases pressure drop.

2.1. *Experimental setup*

A schematic representation of the experimental setup necessary to the operation and analysis of the reforming reactor is presented in Fig. 4. The reactants were fed by a conventional automotive fuel injection system composed of an electric pump, a filter, a mechanical pressure regulator and an automotive solenoid fuel injector, which was operated in PWM mode at an injection pressure of 3.5 bar(g). A Siemens FC300 DN4 Coriolis flow meter was employed to determine the instantaneous glycerol/water flow rate, as well as to provide feedback to a programmable fuel injection used for controlling the reactor feed in set points ranging from 20 to 65 ml/min, with a reproducibility limit of ±0.49 ml/min. Custom inconel K-type thermocouple probes monitored the temperatures in the reactor inlet and outlet points, as well as in the combustion gases circuit. The bed and engine exhaust absolute pressures were measured with piezoresistive transducers

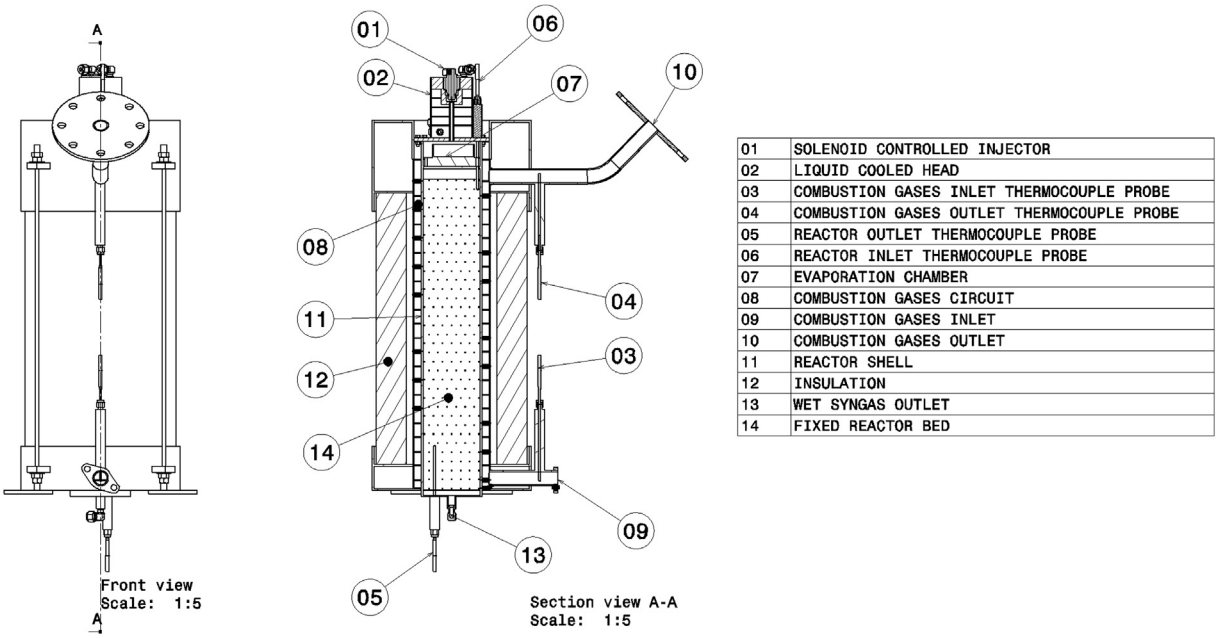

Fig. 2 – Assembly design of the heat recovery steam reforming reactor.

(Omega PXM409). The engine exhaust gas flow was computed with ±26.74 g/min uncertainty from combined measurements conduced with an Omega FMA-900-V gas flow meter and a Siemens FC300 fuel flow meter.

After leaving the reforming reactor, the wet syngas was directed to a liquid separator where the condensate flow composed of tar and water was extracted, measured and conveyed to a total carbon analysis (HACH Spectrophotometer DR 2800 with MR direct method). The condenser is composed by a cylindrical bed of 0.9 dm^3 filled with the reactor's packing material and encircled by a mechanical agitated ice bath. A small gas stream before the exhaust blower was sent to a gas chromatograph (Varian CP 3800) in order to conduct a composition analysis. A thermal conductivity detector (TCD) was used for hydrogen and carbon monoxide analysis, whereas carbon dioxide and light hydrocarbons were computed by a flame ionization detector (FID) detector at 350 °C of oven temperature, employing a capillary column – CP-Sil 5 CB. The variability observed in the mole fractions obtained by the gas chromatography analysis was inferior to 2%.

Table 2 – Engine characteristics.

Configuration	Single cylinder naturally aspirated
Cycle	4 stroke
Injection system	Mechanical – direct injection
Bore × stroke [mm]	78 × 62
Compression rate	23:1
Adopted fuel	Soybean oil methyl ester
Maximum brake power [kW]	4,25 @ 3694 rpm
Thermal efficiency at maximum brake power	19.37%

Both the reactants flow rate and the temperature of the combustion gases delivered to the reactor were monitored and commanded by an automated dynamometric bench. The engine was maintained in fixed speed mode at 3694 rpm, while the dynamometer torque was controlled to attain the prescribed values of bed outlet temperature with a reproducibility of around ±10 K. The data acquisition and control system was composed of a National SCXI system fitted with analog input, frequency input, thermocouple input and analog output cards, while the user interface was implemented with the LabView software.

Five reactant concentrations of glycerol in water, by weight, were considered: 10%, 30%, 50%, 70% and 90%. Each one of these concentrations corresponded to a continuous experimental run where the reactor outlet temperature was varied from 600 °C to 800 °C with intervals of 50 °C. The reactants flow rate was controlled for every experimental condition, for the sake of maintaining a fixed residence time of 4 s based on the thermodynamic state of the water vapor at the reactor outlet. Before an experimental run, the packing material was cleaned, dried, weighted and mounted inside the reactor. Water was injected while heating the reactor to the initial outlet bed temperature of 600 °C, thereafter, the system operated for at last 4 min with the water/glycerol mixture flowing at controlled injection rate in each prescribed step for the bed outlet temperature. A weak water flow was used to flush and cool down the reactor at the end of each run. The reactor packing was then removed, dried and weighted to determine the amount of char. Carbon balances were performed in order to check the reliability of the individual experimental runs, with carbon closures in the range of 97.47 ± 1.94%.

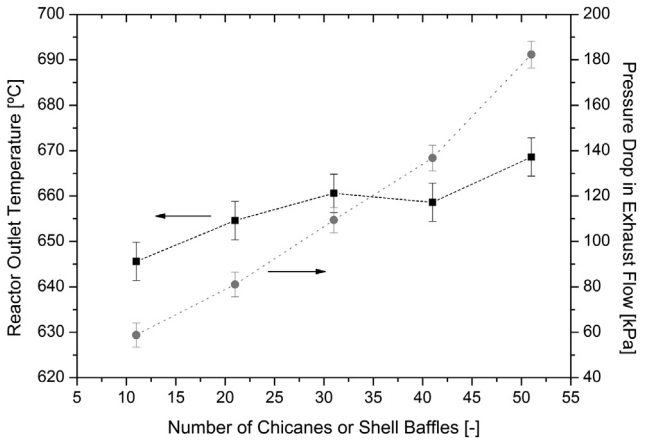

Fig. 3 – Combustion gases pressure drop and reactor outlet temperature for multiple shell configurations.

2.2. *Experimental data assessment*

The gaseous products yield, or steam reforming efficiency (SRE), is defined as:

$$SRE = \frac{m_P}{m_G} = 1 - \frac{m_{WTC}}{m_G} \quad (1)$$

where m_P is the total mass of syngas, m_G is the total mass of glycerol and m_{WTC} is the total mass of water, tar and solid carbon (non-gaseous products) formed in a given experimental condition.

Data presented to the syngas lower heat value (LHV_S) were normalized with relation to the feedstock energy content, being calculated from:

$$LHV_S = \frac{SRE(\sum LHV_i x_i)}{LHV_G} \quad (2)$$

in this equation, LHV_G is the glycerol lower heat value, whereas LHV_i and x_i stand for the lower heat value and experimental mass fraction of the ith component in the gaseous products mixture, respectively. The syngas was modeled as an ideal gas mixture and the enthalpies of each component were taken from the JANAF tables [26].

The energy extracted from the engine exhaust gas stream per kilogram of glycerol was determined in function of temperature, pressure and mass flow data adopting:

$$Q_E = \frac{m_E(h_{E,i} - h_{E,o})}{m_G} \quad (3)$$

where m_E is the totalized mass of exhaust gas that crossed the reactor sleeve in a given experimental condition. The exhaust gas inlet ($h_{E,i}$) and outlet ($h_{E,o}$) enthalpies were computed by employing the PER and EQMD routines [27], with the fuel–air equivalence ratio, pressure and temperature as inputs. Finally, the cold gas efficiency can be expressed as follows:

$$CGE = LHV_S - Q_E \quad (4)$$

As defined here, the cold gas efficiency represents the neat amount of the feedstock heat value that is recovered in terms of cold gaseous products heat value, discounting the energy (heat) extracted from the engine combustion gases. In other words, the CGE value indicates the amount of the feedstock heat value that would be recovered in terms of syngas if the reforming reactions were sustained by burning a part of this product inside the reactor, instead of extracting the energy necessary from the engine combustion gases.

Chemical equilibrium analysis does not take into account the transport and finite rate chemistry phenomena that are present in the system under study. Notwithstanding, results from thermodynamic calculations are used here with two qualitative purposes: as a theoretical benchmark for the final syngas composition and for the identification of kinetic effects, signed by departures between experimental and equilibrium products concentrations. The CEA code (Chemical Equilibrium with Applications) [28] is adopted in order to compute equilibrium compositions for the products of glycerol steam reforming; the results being presented in Section 3 (Figs. 6 and 7). Solid carbon (graphite) and CO, CO_2, CH_4, C_2H_4, H_2 and H_2O as gaseous components were considered in this equilibrium calculations. Ethylene was taken into account here due to its presence in the experimental reforming products, yet near zero equilibrium mole fractions were predicted to this alkene.

3. Reaction pathways and equilibrium syngas composition

Jones and co-workers identified formaldehyde, acetaldehyde and acrolein as the key intermediate products of glycerol steam reforming at 650–700 °C [12]. Using nitric oxide as a radical inhibitor, these authors suggested two concurrent reaction paths dominating the first steps of glycerol decomposition: a radical initiated reaction path for the formation of acrolein (affected by the inhibitor) and a carbon–carbon bond cleavage reaction path for the formation of acetaldehyde (unaffected by the inhibitor). These two reactions are represented, respectively, by pathways 1 and 2 in the simplified scheme of Fig. 5.

Path 1 corresponds to the so-called glycerin dehydration and the acrolein formed in this step, by its turn, is known to rapidly decompose into carbon monoxide, ethylene, propylene, hydrogen and methane, here enumerated in order of importance as regards the molar yield [29]. Carbon–carbon bond cleavage (pathway 2) leads to the formation of formaldehyde and acetaldehyde as intermediate condensables, further decomposed to generate carbon monoxide, hydrogen and methane as gaseous products [30,31].

Reactions involving gaseous products and water are also expected to have influence over the final syngas composition, being represented in the lower part of the scheme depicted in Fig. 5. Methane is formed in detriment of hydrogen through carbon monoxide and carbon dioxide methanation reactions, whereas hydrogen can be obtained from carbon monoxide by means of the water–gas shift reaction [32]. The influences of reaction zone temperature and water concentration on the CH_4 and H_2 yields can be explored, at least qualitatively, by considering that such reactions would proceed to chemical equilibrium conditions, which correspond to the results presented in Figs. 6 and 7. High methane production is

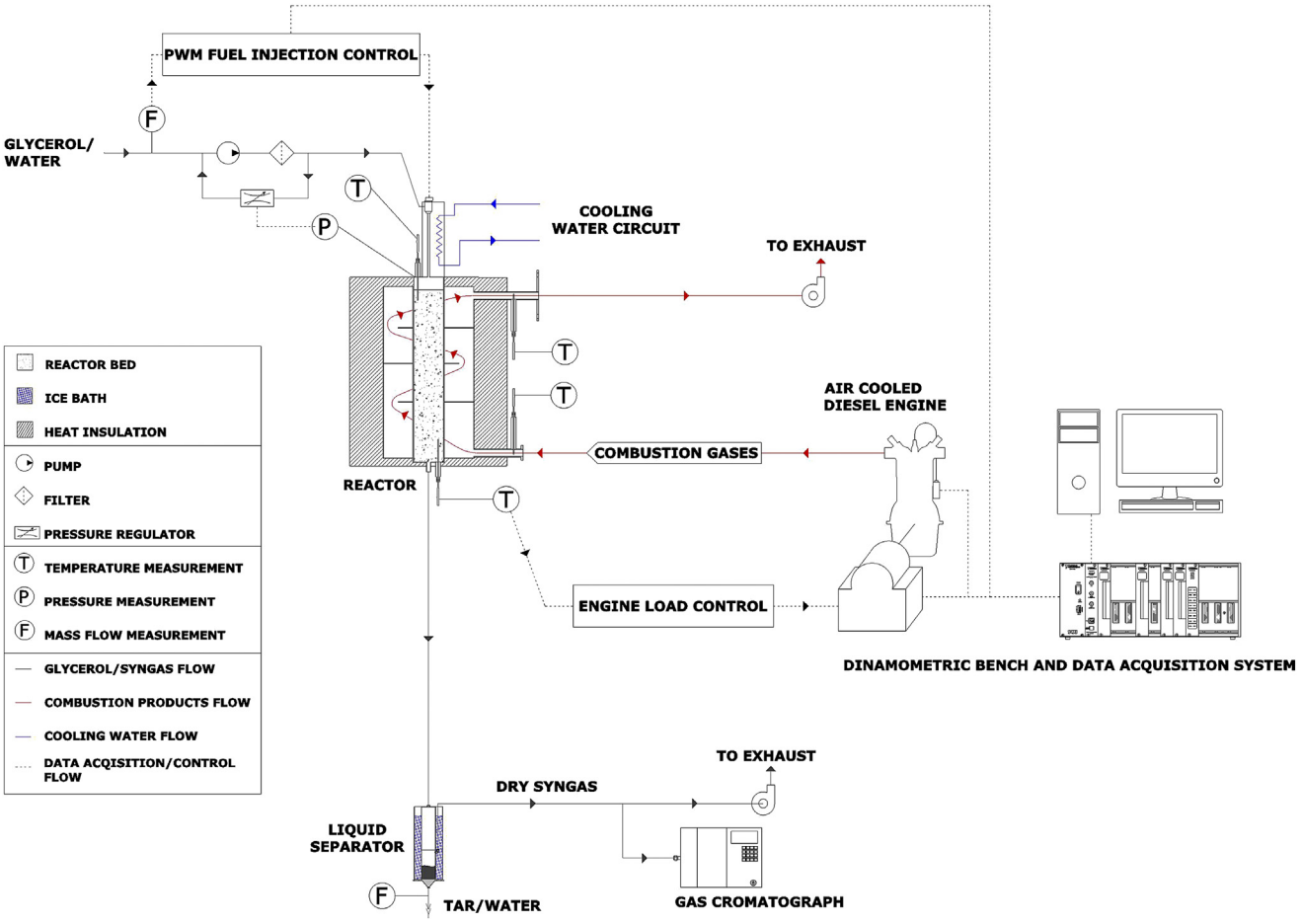

Fig. 4 – Simplified representation of the experimental setup.

predicted at low temperature regimes, where methanation is favored with relation to water–gas shift reaction, as can be seen by Fig. 8. Conversely, methanation reactions become unfeasible from 600 °C giving space to reverse methanation reactions and hydrogen dominates the equilibrium syngas composition in higher temperatures. According to Le Chatelier's Principle, increasing water concentration also changes the equilibrium towards hydrogen, since water participates in the water–gas shift reaction as a reactant and takes part of both methanation reactions as a product. Some minor reduction in methane is observed at glycerol feed concentrations above 60% and low temperatures, as a consequence of the competition with solid carbon (graphite) formed within these operational conditions.

4. Results and discussion

Steam reforming efficiency, cold gas efficiency, syngas heat value, hydrogen and other compounds yields have been analyzed at different temperatures and glycerol to water feed ratios. Steam reforming of glycerol produced a stream rich in H_2, CH_4 and CO with minor amounts of CO_2 and C_2H_4. Temperatures from 239.2 to 356.1 °C were achieved at the top of the reactor bed during the experiments, guaranteeing that the reactants mixture left the evaporation pre-chamber in a superheated vapor state.

4.1. *Steam reforming efficiency and solid carbon formation*

Glycerol steam reforming is a more exergonic reaction than the pyrolysis decomposition one, particularly at mid to lower temperatures, as can be seen in Fig. 1. This suggests that the presence of water enhances a gasification process occurring at gradually increased temperature, as in the case of countercurrent heat exchange. Hence, overall steam reforming efficiencies (SRE) of 94.4%, 91.2%, 79.6%, 72.6% and 28.6% were registered in the experimental runs corresponding to 10%, 30%, 50%, 70% and 90% of glycerol in water, respectively. One can also note that the overall SRE decreased linearly with glycerol mass fraction (x_G) for feed concentrations up to 70%, according to

$$SRE = 99.85 - 0.385x_G \quad (5)$$

with a correlation coefficient of −0.980 and a standard deviation of 2.45. Conversely, a sudden reduction of efficiency was observed in the experimental run with 90% of glycerol. This result exposes a practical difficulty in conducting the thermal decomposition of the glycerol with water as a limiting

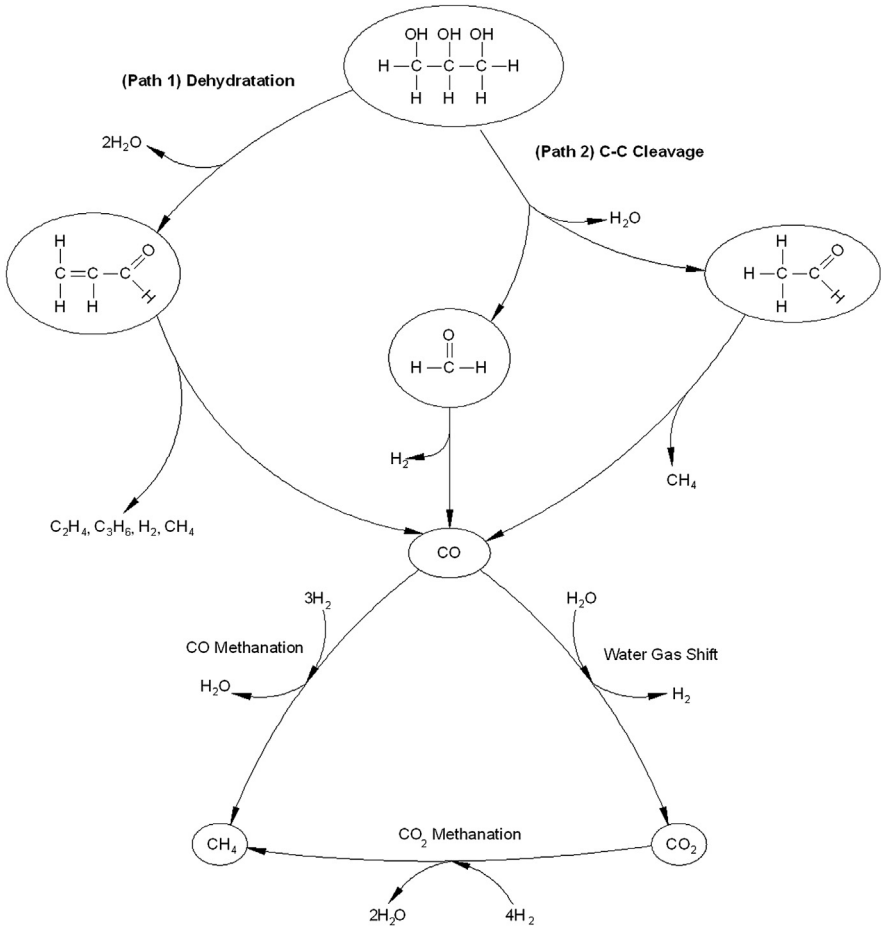

Fig. 5 – Reaction pathways during glycerol reforming process.

reactant for the wet reforming reactions while the parallel pyrolysis reactions are restricted by low temperature conditions.

Individual data obtained for SRE within each stabilized temperature regime are depicted in Fig. 9. Whereas the variation of SRE versus temperature remained inside the uncertainty margin up to 50% of glycerol feed, some improvement can be noticed for the 70 and 90% cases at outlet bed temperatures higher than 700 °C. These results suggest that the gasification of the 90% glycerol mixture would demand higher temperatures than the ones achieved here to be effective.

Even distributions of solid carbon were observed through the radial and axial sections of the reactor for all experimental runs. From Fig. 10, it can be noticed that the production of char was restricted by increasing the reactor water feed, a practical measure with extensive use in industry. Except for the 90% glycerol experimental run, the results obtained with the heat recovery reactor for solid carbon and SRE did not differ significantly from the ones reported in the literature for homogeneous temperature conditions (see Table 1).

4.2. *Syngas composition and heat value*

Gas chromatography results are presented in Table 3. Hydrogen, methane and carbon monoxide predominated among the products from the glycerol steam reforming, with carbon dioxide and ethylene appearing in minor amounts. The gaseous composition obtained in the 90% glycerol run demanded temperatures above 700 °C to become representative when compared to other regimes, due to the ineffective reforming process addressed in Section 4.1.

As anticipated by the chemical equilibrium analysis, methane is favored under experimental conditions characterized by low temperatures and high glycerol feed concentrations. Methane mole fractions ranging from 25 to 40% and increasing with the glycerol feed concentration were registered in the experiments at 600 °C of reactor outlet temperature, whereas these mole fractions fell to around 20% when the reactor outlet temperature was raised to 800 °C. In spite of the qualitative agreement, such methane concentrations are significantly higher than the corresponding equilibrium predictions and, in fact, would be equivalent to equilibrium states with temperatures about 250 °C lower than the ones acquired at the reactor outlet. These departures indicate that methane formed in the preliminary steps of glycerol decomposition, which take place in relatively low temperatures at the reactor top, would demand a period higher than the effective residence time to be decomposed by reverse methanation reactions or, in other words, that methane consumption is controlled by slow kinetics reactions.

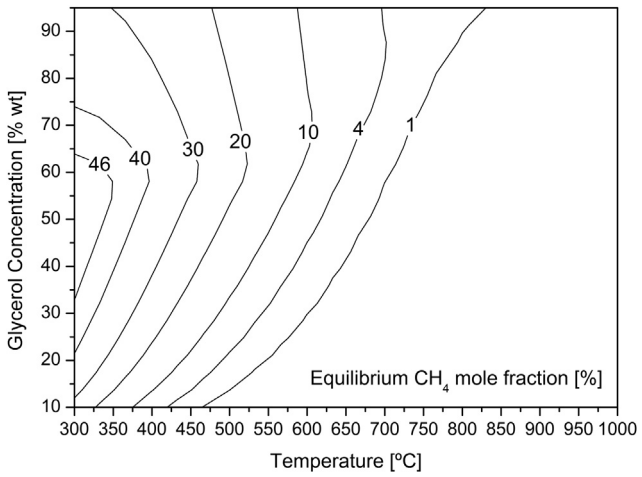

Fig. 6 – Chemical equilibrium concentrations of methane on dry basis.

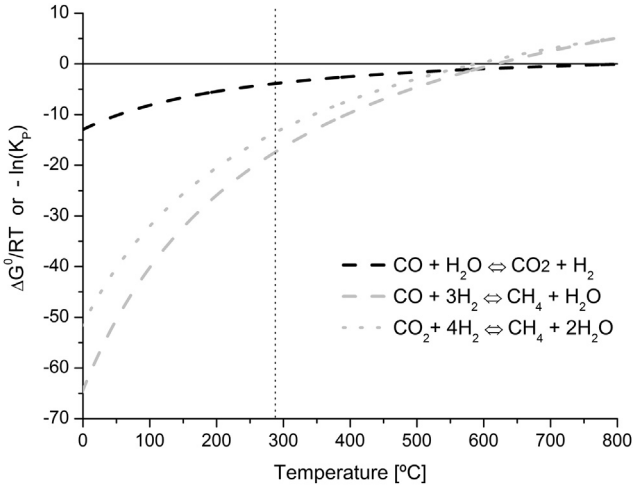

Fig. 8 – $\Delta G^0/RT$ versus temperature for methanation and water–gas shift reactions.

Non-equilibrium ethylene formed through glycerol dehydration (PATH I) was also persistent among the final gaseous products. Radical initiated reactions such as the ones present in glycerol dehydration are favored by high temperature conditions and, thus, ethylene mole fractions increased from trace amounts to 3.5% with temperature and glycerol feed concentration.

Hydrogen yield increased with temperature according to the thermodynamic predictions but, surprisingly, was quite unaffected by feed water concentration down to the limit of 30%. Besides the water–gas shift reaction involving final reforming products, free radical metathesis reactions of H-atoms with glycerol can also have contributed to the formation of hydrogen at elevated temperatures [33]. With outlet bed temperatures above 700 °C, moderate to high hydrogen concentrations were obtained here (36–54%) when compared to the literature data, which ranges from 22 to 68%. The maximum hydrogen mole fraction of 54% was attained with 50% of glycerol feed at an outlet bed temperature of 800 °C and a SRE of 81.5%. This data corresponded to a yield of 71 mg_{H_2}/g_G, which is equivalent to 61.84% of the equilibrium benchmark.

The operational map obtained for the lower heat value of the reforming products is depicted in Fig. 11. The fundamental role of the hydrogen yield upon the reforming gas heat value is evident in this figure, where a normalized lower heat value level of 140% is exhibited in the hydrogen rich region delimited by outlet bed temperatures above 700 °C and glycerol feed concentrations within 50–70%. On the contrary, limited syngas heat values of around 60% were obtained at low temperature or 90% glycerol feed, conditions where CO was the dominant gaseous product.

4.3. *Bed temperature profile*

To obtain further insight into the effects of the heat recovery reactor configuration on the syngas composition, a comparison with a forced isothermal condition was also conducted.

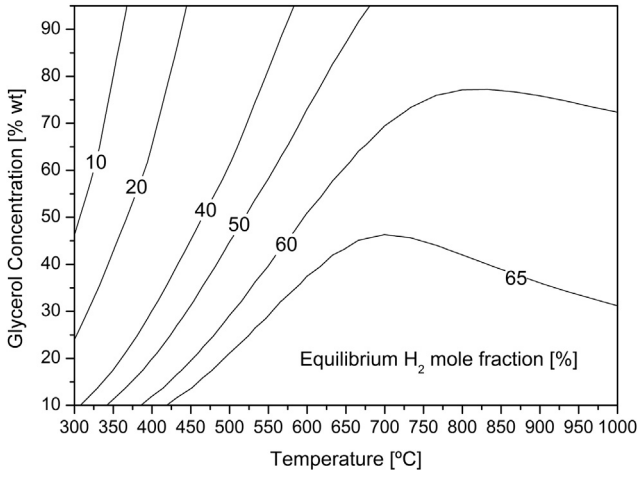

Fig. 7 – Chemical equilibrium concentrations of hydrogen on dry basis.

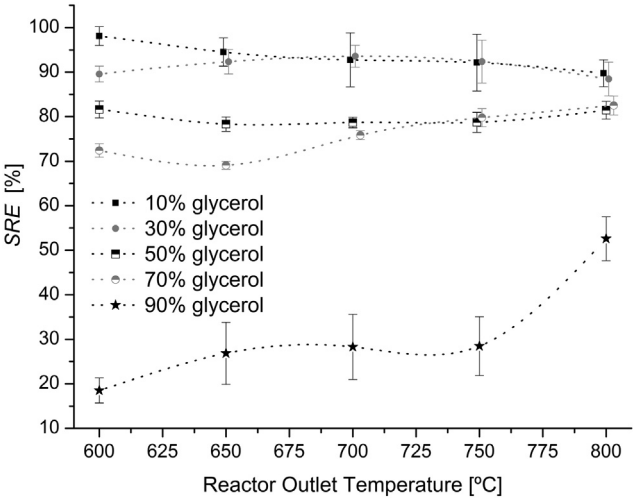

Fig. 9 – Steam reforming efficiencies versus reactor bed outlet temperature.

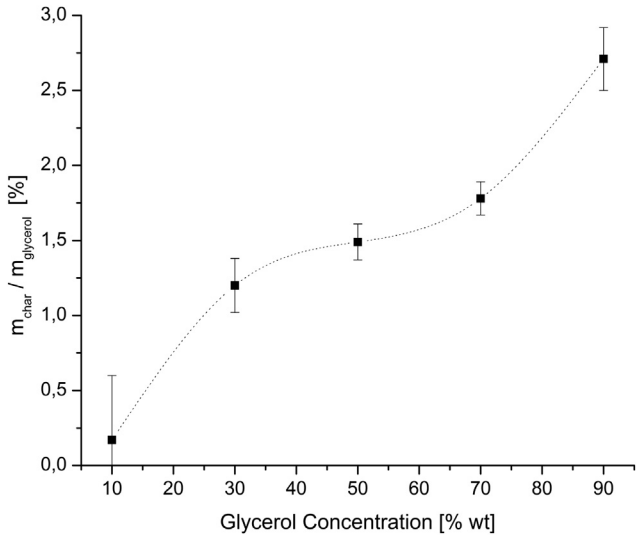

Fig. 10 – Overall solid carbon production for each experimental run.

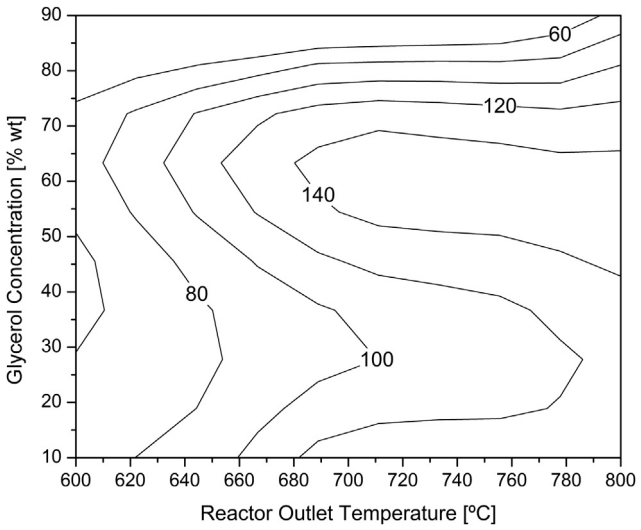

Fig. 11 – Normalized syngas heat value [% of feedstock heat value] obtained for the heat recovery steam reforming of glycerol.

The quasi-isothermal experiments were run with the replacement of the external insulator by an Omega CRFC-524/240-A heater, while the hot gas side of the heat exchanger was completely filled with quartz sand.

As can be seen from Table 4, heat recovery hydrogen data correspond to around 85% of the isothermal yield. On the other hand, methane and ethylene productions significantly exceeded the isothermal benchmark. These results are in agreement with the preceding theoretical analysis, since the lower temperatures at the reactor top with relation to the isothermal cases are expected to increase methane and ethylene yields, in detriment of the hydrogen production.

Table 3 – Mole fractions of the gaseous species produced from heat recovery glycerol steam reforming.

Operational conditions		Gas products concentration [%mol]				
Glycerol feed ratio [%wt]	Outlet bed temperature [°C]	CO_2	CH_4	CO	H_2	C_2H_4
10	600	30.0	25.5	29.0	15.4	0.0
	650	22.6	26.6	25.8	23.9	0.1
	700	11.2	20.2	18.8	48.5	0.3
	750	10.5	19.4	19.6	48.9	0.7
	800	9.7	18.5	18.3	50.6	2.0
30	600	24.9	26.4	42.8	5.9	0.0
	650	22.6	25.0	31.2	20.6	0.2
	700	20.4	24.5	19.7	35.2	0.2
	750	15.1	20.7	23.2	40.3	0.7
	800	7.2	17.6	26.8	46.1	2.3
50	600	20.8	32.2	38.6	7.8	0.6
	650	9.5	31.5	28.4	30.0	0.6
	700	9.2	31.0	14.5	44.0	1.4
	750	6.8	27.5	16.8	47.5	1.5
	800	4.8	19.8	19.0	54.0	2.4
70	600	13.4	39.7	33.5	11.2	2.3
	650	8.2	39.9	17.2	31.2	3.4
	700	6.7	39.0	10.6	40.4	3.4
	750	7.3	21.7	17.3	50.4	3.3
	800	5.3	16.9	24.1	50.7	3.0
90	600	45.5	4.2	50.0	0.3	0.0
	650	30.5	12.6	54.9	1.6	0.4
	700	9.5	21.4	62.6	5.1	1.5
	750	4.5	25.8	60.1	8.0	1.6
	800	1.4	24.8	52.1	15.3	6.5

Table 4 – Mole fractions of the gaseous species resulting from glycerol steam reforming experiments at 800 °C of outlet bed temperature.

Operational conditions		Gas products concentration [%mol]					
Glycerol feed ratio [%wt]	Bed temperature profile	Inlet bed temperature [°C]	CO_2	CH_4	CO	H_2	C_2H_4
10	Quasi-isothermal	631	7.8	4.5	25.6	61	1.1
	Heat recovery	252	9.7	18.5	18.3	50.6	2
30	Quasi-isothermal	719	6.8	5.8	29.1	57	1.3
	Heat recovery	296	7.2	17.6	26.8	46.1	2.3
50	Quasi-isothermal	744	4.5	5.4	29.8	58.6	1.7
	Heat recovery	341	4.8	19.8	19	54	2.4

4.4. *Cold gas efficiency*

The balance between the syngas heat value and the amount of heat recovery demanded by the steam reforming reactions is addressed here by means of the cold gas efficiency. Negative values of this parameter indicate an energy consumption superior to the syngas heat value, while positive values characterize operational regimes where the reforming reactions could be sustained by burning part of the generated syngas, instead of using a heat recovery strategy.

Feed concentration is an important efficiency consideration, since either heating more water than is necessary or restricting the reforming reactions due to low water concentration are not desirable. Other factors with negative efficiency effects are the energy waste associated to char and tar effluents and insulation heat losses in the hot gas circuit. The cold gas efficiencies obtained in the experiments for the heat recovery steam reforming of glycerol are shown in Fig. 12. Negative values of CGE predominated for the two extrema cases of 10 and 90% glycerol feeds. The first one is an example of the detrimental effects of excessive water feed, where 86–89% of the heat recovered from the exhaust gases was compromised in water heating up. Conversely, the low water concentration constrained the heat value of the syngas obtained for the 90% glycerol feed case.

Positive, yet moderate, CGE values were obtained with 30% glycerol in water from 650 °C and the energy expending associated to water heating up fell to 75–64% of the heat recovery within this experimental run. This figure improved considerably in the 50 and 70% glycerol feed cases, which exhibited positive efficiencies directly from 600 °C and a stable CGE level of 85% in temperatures above 700 °C. From the point of view of energy efficiency, 70% of glycerol feed at an outlet bed temperature of 750 °C was the best operational condition achieved here, with a cold gas efficiency of 87%.

5. Conclusions

Glycerol was successfully gasified using a heat recovery reactor that provided hydrogen and methane rich gaseous products. The reactor configuration used here consists of a fixed porous bed mounted in the tube side of a specially designed heat exchanger, with combustion gases circulating in a shell sleeve with 22 passes. This arrangement caused the steam reforming reactions to proceed at gradually increased temperature conditions; starting at around 300 °C in the top section of the reactor bed and finishing in a controlled outlet bed temperature of 600–800 °C. The main discrepancy observed here in comparison to data reported for homogeneous temperature reactors was the persistence, among the final products, of methane and ethylene formed in relative low temperatures at the top of the reactor bed.

It was noticed in the experiments that the steam reforming efficiency linearly decreased with increasing the glycerol feed concentration up to the limit of 70% in water, whereas an abrupt efficiency drop indicating a poor gasification performance was registered only in the experimental run with 90% of glycerol. Methane concentration in the gaseous products ranged from 20 to 40% according to the glycerol feed in the experiments at 600 °C of reactor outlet temperature, falling to around 20% when the reactor outlet temperature was raised to 800 °C.

Hydrogen predominated from 700 °C and a maximum hydrogen mole fraction of 54% was attained with 50% of glycerol feed and outlet bed temperature of 800 °C, corresponding to 61.84% of the equilibrium benchmark production. The hydrogen rich region delimited by outlet bed temperatures above 700 °C and glycerol feed concentrations within 50–70% offered the best operational conditions with regards to energy efficiency, where a syngas with normalized lower heat values of about 140% was produced at a stable cold gas efficiency level of 85%.

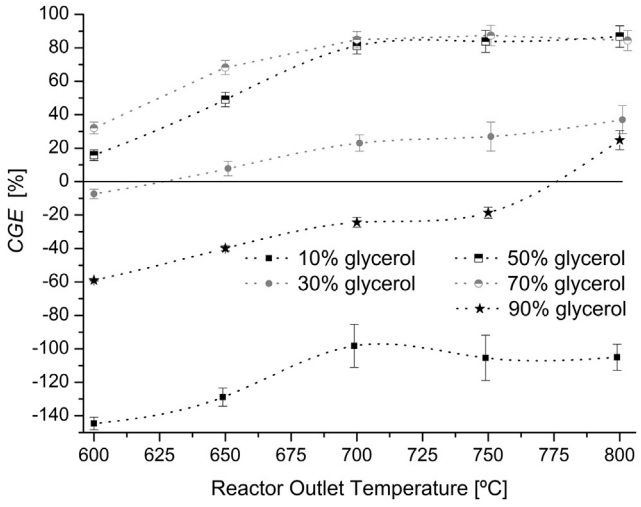

Fig. 12 – Cold gas efficiencies obtained for the heat recovery steam reforming of glycerol.

Acknowledgments

This research was partially supported by the Brazilian National Council for Scientific and Technological Development (CNPq) under Grant No 574640/2008-8.

REFERENCES

[1] Grabosky MS, McCormick RL. Combustion of fat and vegetable oil derived fuels in diesel engines. Prog Energy Combust Sci 1998;24(2):125–64.
[2] Agarwal AK. Biofuels (alcohols and biodiesel) applications as fuels for internal combustion engines. Prog Energy Combust Sci 2007;33(3):233–71.
[3] Demirbas A. Progress and recent trends in biofuels. Prog Energy Combust Sci 2007;33(1):1–18.
[4] Leoneti AB, Leoneti VA, de Oliveira SVWB. Glycerol as a by-product of biodiesel production in Brazil: alternatives for the use of unrefined glycerol. Renew Energy 2012;45:138–45.
[5] Pachauri N, He B. Value-added utilization of crude glycerol from biodiesel production: a survey of current research activities. ASABE 2006. ASABE Paper No. 066223.
[6] Silva GP, Mack M, Contiero J. Glycerol: a promising and abundant carbon source for industrial microbiology. Biotechnol Adv 2009;27:30–9.
[7] Fernando SD, Adhikari S, Kota K, Bandi R. Glycerol based automotive fuels from future biorefineries. Fuel 2007;86:2806–9.
[8] Rahmat N, Abdullah AZ, Mohamed AR. Recent progress on innovative and potential technologies for glycerol transformation into fuel additives: a critical review. Renew Sustain Energy Rev 2010;14:987–1000.
[9] Davda RR, Shabaker JW, Huber GW, Cortright RD, Dumesic JA. A review of catalytic issues and process conditions for renewable hydrogen and alkanes by aqueous-phase reforming of oxygenated hydrocarbons over supported metal catalysts. Appl Catal B Environ 2005;56:171–86.
[10] Adhikari S, Fernando SD, Haryanto A. Hydrogen production from glycerol: an update. Energy Convers Manag 2009;50(10):2600–4.
[11] Sarma SJ, Brar SK, Sydney EB, Bihan YL, Buelna G, Socol CR. Microbial hydrogen production by bioconversion of crude glycerol: a review. Int J Hydrogen Energy 2012;37:6473–90.
[12] Stein YS, Antal Jr MJ, Jones Jr M. A study of the gas-phase pyrolysis of glycerol. J Anal Appl Pyrolysis 1983;4(4):283–96.
[13] Valliyappan T, Ferdous D, Bakhshi NN, Dalai AK. Production of hydrogen and syngas via steam gasification of glycerol in a fixed-bed reactor. Top Catal 2008;49:59–67.
[14] Adhikari S, Fernando SD, Haryanto A. Hydrogen production from glycerin by steam reforming over nickel catalysts. Renew Energy 2008;33:1097–100.
[15] Fernández Y, Arenillas A, Bermúdez JM, Menéndez JA. Comparative study of conventional and microwave-assisted pyrolysis, steam and dry reforming of glycerol for syngas production, using a carbonaceous catalyst. J Anal Appl Pyrolysis 2010;88(2):155–9.
[16] Atong D, Pechyen C, Aht-Ong D, Sricharoenchaikul V. Synthetic olivine supported nickel catalysts for gasification of glycerol. Appl Clay Sci 2011;53(2):244–53.
[17] Douette AMD, Turn SQ, Wang W, Keffer VI. Experimental investigation of hydrogen production from glycerin. Energy & Fuels 2007;21:3499–504.
[18] Yoon SJ, Choi YC, Son YI, Lee SH, Lee JG. Gasification of biodiesel by-product with air or oxygen to make syngas. Bioresour Technol 2010;101(4):1227–32.
[19] Valliyappan T, Bakhshi NN, Dalai AK. Pyrolysis of glycerol for the production of hydrogen or syn gas. Bioresour Technol 2008;99(10):4476–83.
[20] Cortright RD, Davda RR, Dumesic JA. Hydrogen from catalytic reforming of biomass-derived hydrocarbons in liquid water. Nature 2002;418:964–7.
[21] Huber GW, Shabaker JW, Dumesic JA. Raney Ni-Sn catalyst for H2 production from biomass-derived hydrocarbons. Science 2003;300:2075–7.
[22] Byrd AJ, Pant KK, Gupta RB. Hydrogen production from glycerol by reforming in supercritical water over Ru/Al_2O_3 catalyst. Fuel 2008;87:2956–60.
[23] Xu D, Wang S, Hu X, Chen C, Zhang O, Gong Y. Catalytic gasification of glycine and glycerol in supercritical water. Inter J Hydrogen Energy 2009;34(13):5357–64.
[24] May A, Salvadó J, Torras C, Montané D. Catalytic gasification of glycerol in supercritical water. Chem Eng J 2010;160:751–9.
[25] Guo S, Guo L, Cao C, Yin J, Lu Y, Zhang X. Hydrogen production from glycerol by supercritical water gasification in a continuous flow tubular reactor. Int J Hydrogen Energy 2012;37:5559–68.
[26] JANAF thermochemical tables. 2nd ed.; 1971. NSRDS-NBS 37, U.S. Dep. Of Commerce, June.
[27] Olikara C, Borman GL. A computer program for calculating properties of equilibrium combustion products with some applications to I.C. engines, Society of Automotive Engineers; 1975. SAE Paper 750468.
[28] Mcbride BJ, Gordon S. Computer program for calculation of complex chemical equilibrium compositions and applications I. Analysis. NASA Reference Publication 1311; 1996.
[29] Castro CE, Rust FF. Thermal decomposition of acrolein. The attack of methyl and t-butoxy free radicals on acrolein. J Am Chem Soc 1961;83:4928–32.
[30] Saito K, Kakumoto T, Nakanishi Y, Imamura A. Thermal decomposition of formaldehyde at high temperatures. J Phys Chem 1985;89(14):3109–13.
[31] Freeman GR, Danby CJ, Hinshelwood C. The pyrolytic reactions of acetaldehyde in presence of nitric oxide. Proc Royal Soc London A 1958;245:456–69.
[32] Gao J, Wang Y, Ping Y, Hu D, Xu G, Gu F, et al. A thermodynamic analysis of methanation reactions of carbon oxides for the production of synthetic natural gas. RSC Adv 2012;2:2358–68.
[33] Bühler W, Dinjus E, Ederer HJ, Kruse A, Mas C. Ionic reactions and pyrolysis of glycerol as competing reaction pathways in near- and supercritical water. J Supercritical Fluids 2002;22(1):37–53.